Appl. Phys. A 81, 1083–1088 (2005)
DOI: 10.1007/s00339-004-2960-z

Applied Physics A
Materials Science & Processing

I.A. OVID'KO✉
A.G. SHEINERMAN

Irradiation-induced amorphization processes in nanocrystalline solids

Institute for Problems of Mechanical Engineering, Russian Academy of Sciences, Bolshoj 61, Vas. Ostrov, St. Petersburg 199178, Russia

Received: 17 May 2004/Accepted: 10 June 2004
Published online: 29 July 2004 •

ABSTRACT A theoretical model is suggested which describes irradiation-induced amorphization in nanocrystalline solids, using the rate theory approach. In the framework of the model, interfaces (grain boundaries) cause the two basic effects on irradiation-induced damage and amorphization processes in nanocrystalline solids where the volume fraction of the interfacial phase is extremely large. First, amorphization is enhanced in nanocrystalline solids, because high-density ensembles of interfaces essentially contribute to the total energy of the crystalline state and thereby provide a shift in the energetics of amorphization. Second, interfaces serve as effective sinks of irradiation-produced point defects and thereby hamper amorphization driven by defect accumulation. The competition between these effects is described by kinetic equations for densities of point defects in nanoscale grains in nanocrystalline solids under irradiation treatment. This competition is shown to be responsible for the specific behavior of irradiated nanocrystalline solids, which is different from that of their coarse-grained counterparts. The suggested model accounts for the experimental data reported in the literature.

PACS 61.46.+w; 61.72.Cc; 61.80.Az

1 Introduction

Nanostructured solids exhibit the outstanding physical, mechanical and chemical properties due to nanoscale and interface effects; see, e.g., [1–3]. These properties open a range of new applications of nanostructured solids in high technologies. In particular, single-phase and composite nanocrystalline materials have wide perspectives to be exploited in structural applications and nanoelectronics in various radiation environments in space vehicles, nuclear reactors, etc. Irradiation treatment of conventional coarse-grained polycrystalline and microscale composite solids produces defects in crystal lattices and often induces amorphization (crystal-to-glass transformation); see, e.g., [4–14]. Similar irradiation-induced structural transformations and amorphization are expected to occur in nanocrystalline solids. In doing so, however, damage and amorphization processes can show the specific peculiarities in nanocrystalline solids due to the presence of high-density ensembles of interfaces (grain and interphase boundaries) and other specific structural peculiarities. This statement is supported by experimental observations [15–22] and computer simulations [23–25] of defect production, structural and amorphizing transformations induced by irradiation in nanocrystalline and nanocomposite solids. In particular, following experiments [17, 18], irradiation-induced amorphization is essentially enhanced in nanoparticles (ZrO_2, Si) in nanocrystalline composites compared to their conventional coarse-grained polycrystalline counterparts. For instance, zirconia (ZrO_2) nanoparticles in nanocrystalline composites can be amorphized at a dose as low as 0.9 dpa [17, 18], whereas bulk zirconia has been irradiated to 680 dpa with no evidence of amorphization [26]. At the same time, experiments [15, 16] have shown that nanocrystalline solids (ZrO_2, Pd) are highly resistant to irradiation-induced defect production, compared to coarse-grained polycrystals with the same chemical composition. The defect production, in turn, is commonly responsible for solid state amorphization, in which case experimental data [15, 16] are indirectly indicative of the fact that amorphization processes are hampered in irradiated nanocrystalline solids. Thus, there are intriguing controversial experimental data giving evidence for a rather specific behavior of nanocrystalline solids under irradiation. The main aim of this paper is to suggest a theoretical model describing these controversial experimental data. The model takes into consideration the competing interface effects that simultaneously cause both enhancement and suppression of amorphization processes in nanocrystalline solids under irradiation.

2 Evolution of point defects in nanocrystalline solids under irradiation. Basic statements of the model

Let us consider a nanocrystalline solid under irradiation. We assume that the irradiation treatment occurs with tentatively the same intensity in all the volume of the nanocrystalline solid during some time interval $[0, t_1]$. Nanoscale grains of the solid are modeled as identical spherical balls with the radius a. In the first approximation, irradiation processes in nanocrystalline solids can be divided into the two basic categories: high- and low-energy irradiation processes. High-energy irradiation produces vacancies and self-interstitials in both nanograin interiors and grain boundaries (Fig. 1a). Low-energy irradiation causes the gen-

✉ Fax: +7-812/321-4771, E-mail: ovidko@def.ipme.ru

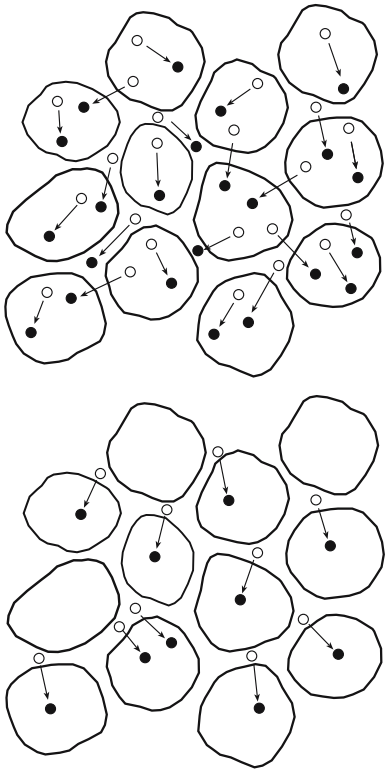

FIGURE 1 Nanocrystalline solid under **a** high- and **b** low-energy irradiation treatment (schematically). Irradiation-produced pairs of vacancies and interstitials are shown as *pairs of open* and *full circles*, respectively, connected by *arrows*. The *closed contours* bound the grains while the space in between the contours represents the grain boundaries

eration of vacancies only in the grain boundary phase (Fig. 1b) where the atomic density and thereby the vacancy formation energy are low compared to those in the bulk (nanograin interiors). At the same time, low-energy irradiation produces interstitial atoms in both nanograin interiors and grain boundaries (Fig. 1b). (In the former case, irradiation causes host atoms to move from their initial sites in grain boundary regions to adjacent nanograin interiors. As a result, vacancies in grain boundaries and interstitials in nanograin interiors are generated.)

Also, we assume that grain boundaries serve as effective sinks of point defects - vacancies and interstitial atoms - that migrate from nanograin interiors towards boundaries. This assumption is supported, for instance, by molecular dynamics simulations [23, 24] showing intense absorption of point defects in nanocrystalline solids under irradiation.

In general, by analogy with the situation with conventional coarse-grained polycrystalline materials, the following transformations of defect structures can occur in nanocrystalline solids under either low- or high-energy irradiation:

(i) irradiation-induced formation of point defects;

(ii) absorption of point defects by grain boundaries;

(iii) annihilation of vacancies and interstitial atoms;

(iv) formation of stable clusters of point defects.

Let us discuss the interface and nanoscale effects on the processes (i)-(iv) in nanocrystalline solids under irradiation. The process (i), the irradiation-induced formation of point defects, is the dominant process responsible for damage in irradiated crystals [4–14]. This process occurs in nanograin interiors in the same way as in conventional microscale grains and thereby is essential in both coarse-grained and nanocrystalline materials. More than that, the irradiation-induced formation of point defects is enhanced in the grain boundary phase where the atomic density and thereby the vacancy formation energy are low compared to those in the bulk phase. At the same time, the volume fraction of the grain boundary phase in nanocrystalline solids is very large. In these circumstances, point defects in nanocrystalline solids are generated under irradiation more intensively than in their coarse-grained counterparts. Also, the process (ii), absorption of point defects by grain boundaries, intensively occurs in nanocrystalline solids, because the volume fraction of the grain boundary phase is extremely large. In addition, the migration path of point defects towards grain boundaries in nanoscale grains is very short. Thus, the processes (i) and (ii) intensively occur and strongly affect evolution of point defects in nanocrystalline solids under irradiation.

At the same time, the annihilation of point defects (process (iii)) is not intense in irradiated nanocrystalline solids due to the interface and nanoscale effects. In particular, as shown below, the density of vacancies in nanograin interiors of a nanocrystalline solid under high-energy irradiation is much higher than that of interstitials. In the case of low-energy irradiation, the density of interstitials in nanograin interiors is much higher than that of vacancies. In these circumstances, the annihilation process (iii) does not significantly affect evolution of point defects in nanocrystalline solids under irradiation.

In order to illustrate the above statement, first, let us consider the case of high-energy irradiation. In this case, owing to inelastic collision events, vacancies and interstitials are generated in both nanograin interiors and grain boundaries (Fig. 1a). Interstitials generated in nanograin interiors and characterized by a relatively high mobility rapidly migrate towards grain boundaries where they are absorbed [23, 24, 27]. Therefore, after some time interval (exceeding the mean time that characterizes migration of interstitials from nanograins towards grain boundaries), the concentration of interstitials becomes low compared to the concentration of slow vacancies in irradiated nanocrystalline solids. As a corollary, the point defect annihilation is not intense in nanocrystalline solids under high-energy irradiation.

In the case of low-energy irradiation, vacancies are formed mostly in grain boundaries, while interstitials generated in inelastic collisions of host atoms and irradiation particles can move from grain boundaries to nanograin interiors (Fig. 1b). (In doing so, we assume that interstitials move to all regions of nanograin interiors but not only to the regions in vicinities of grain boundaries.) In these circumstances, the density of interstitials in nanograin interiors is much higher than that of vacancies in irradiated nanocrystalline solids. As a corollary, the point defect annihilation is not intense in nanocrystalline solids under low-energy irradiation.

Now let us consider the process (iv), the formation of clusters of point defects. This process does not play a significant role, because amorphization occurs in nanocrystalline solids at a critical defect density being lower than the density sufficient for intense formation of point defect clusters.

More precisely, the point defect clusters are hardly formed, if $zn(a/b)^2 \ll 1$, where n is the relative concentration of point defects of one type (vacancies or interstitials), z is the number of the nearest neighboring atoms for an atom in the crystal lattice, and b is the interatomic distance. At the same time, the critical concentration of point defects for amorphization is low in nanocrystalline solids where grain boundaries provide a shift in the energetics of amorphization. As shown in next sections, typical values of the critical concentration for amorphization obey the inequality $zn(a/b)^2 \ll 1$, in which case amorphization prevents the formation of point defect clusters in irradiated nanocrystalline solids.

To summarize, with the specific structural features of nanocrystalline solids, the only processes (i) and (ii) crucially affect evolution of point defects in such solids under irradiation. The processes (iii) and (iv) are not essential due to the interface and nanoscale effects. Therefore, in the framework of our first approximation model, we will focus our analysis on the only processes (i) and (ii) in irradiated nanocrystalline solids.

3 Evolution of point defects and amorphization in irradiated nanocrystalline solids. Model equations

Let us describe the evolution of point defect ensembles in nanocrystalline solids under irradiation. In doing so, we will use both representations of our first approximation model developed in the previous section and rate theory methods [28–31] effectively exploited in a theoretical description of damage and amorphization processes in conventional coarse-grained polycrystalline solids. The two basic processes that control evolution of point defects are taken into account in the rate-theory equations for densities of vacancies and interstitials in irradiated nanocrystalline solids. These processes are (i) the irradiation-induced generation of point defects and (ii) migration of point defects from nanograin interiors towards grain boundaries where defects are absorbed.

Let γ be the mean number of interstitials produced by irradiation in a unit volume of a material per unit time interval. In the situation with high-energy irradiation, γ is a constant value which depends on both irradiation intensity and energy of irradiation particles; γ is independent on nanograin size a. For low-energy irradiation treatment, γ is proportional to the volume fraction F of the grain boundary phase in a nanocrystalline solid. That is, $\gamma = \beta F$, where β is the factor taking into account irradiation intensity and energy. In the framework of our model, grain boundaries represent spherical shells of thickness h. They surround ball-like nanograins with radius a. In this case, we have: $F = 3\,h/a$, and $\gamma = 3\,h\beta/a$.

Let us calculate the mean concentration of point defects in a nanocrystalline solid under irradiation treatment. Let $t = 0$ and $t = t_1$ be respectively the initial and final time moments of irradiation treatment. In the framework of our model representing nanograins as ball-like regions, the concentration c of point defects at a time moment t in a point of the nanocrystalline specimen depends on t and the distance r between this point and the center of the nanograin containing the point. That is, $c = c(r, t)$.

The behaviors of the absolute concentration $c(r, t)$ of point defects (vacancies in the case of high-energy irradiation and interstitials in the case of low-energy irradiation) in nanograin interiors are very different during and after irradiation treatment. Therefore, we consider these cases separately. To do so, let us designate the point defect concentration as $c_1(r, t)$ during irradiation treatment (for $t \in [0, t_1]$) and $c_2(r, t)$ after irradiation treatment (for $t > t_1$). During irradiation treatment, the concentration c_1 in nanograins evolves due to both the irradiation-induced generation of point defects and their migration towards grain boundaries. Irradiation increases c_1 by the quantity γ per unit time. Defect migration towards grain boundaries causes the change of the concentration c_1 (per unit time) by value of $D\Delta c_1$ [32], where D is the diffusion coefficient, and Δ is the Laplace operator. In the considered case of spherical symmetry, we have $\Delta c_1 = \frac{1}{r^2}\frac{\partial}{\partial r}\left(r^2\frac{\partial c_1}{\partial r}\right)$. With the assumption that grain boundaries absorb all point defects reaching them, the boundary condition at grain boundaries is given as: $c_1(r = a) = 0$.

Thus, the concentration c_1 as a function of r and t may be found as a solution of the following equation with mixed initial and boundary conditions:

$$\frac{\partial c_1}{\partial t} = \gamma + \frac{D}{r^2}\frac{\partial}{\partial r}\left(r^2\frac{\partial c_1}{\partial r}\right), \quad 0 \le r < a, \quad 0 < t \le t_1, \tag{1}$$

$$c_1(r = a) = 0, \quad c_1(t = 0) = 0. \tag{2}$$

The concentration c_2 of point defects in a nanocrystalline solid after irradiation treatment ($\gamma = 0$) evolves due to migration of these defects towards grain boundaries where they are absorbed. In this situation, $c_2(r, t)$ obeys the following equation with mixed initial and boundary conditions:

$$\frac{\partial c_2}{\partial t} = \frac{D}{r^2}\frac{\partial}{\partial r}\left(r^2\frac{\partial c_2}{\partial r}\right), \quad 0 \le r < a, \quad t > t_1, \tag{3}$$

$$c_2(r = a) = 0, \quad c_2(t = t_1) = c_1(t = t_1). \tag{4}$$

With the replacement of variables: $c_1 = \tilde{c}_1 - \gamma(r^2 - a^2)/(6D)$, the system (1) and (2) is reduced to the standard system:

$$\frac{\partial \tilde{c}_1}{\partial t} = \frac{D}{r^2}\frac{\partial}{\partial r}\left(r^2\frac{\partial \tilde{c}_1}{\partial r}\right), \quad 0 \le r < a, \quad 0 < t \le t_1, \tag{5}$$

$$\tilde{c}_1(r = a) = 0, \quad \tilde{c}_1(t = 0) = \frac{\gamma}{6D}(r^2 - a^2). \tag{6}$$

It is effectively solved by the method based on separation of variables. In doing so, we find the solution of (1) and (2) to be as follows:

$$c_1(r, t) = -\frac{\gamma a^2}{6D}\left\{1 - \frac{r^2}{a^2} + \frac{12a}{\pi^3 r}\sum_{n=1}^{\infty}\frac{(-1)^n}{n^3}\sin\frac{\pi n r}{a} \times \exp\left(-\frac{\pi^2 n^2}{a^2}Dt\right)\right\}. \tag{7}$$

Substitution of solution (7) into the second equation from (4) yields the initial condition for (3). With conditions (4), we find the solution of (3) to be given as:

$$c_2(r,t) = -\frac{2\gamma a^3}{D\pi^3 r}\sum_{n=1}^{\infty}\frac{(-1)^n}{n^3}\left[1-\exp\left(-\frac{\pi^2 n^2}{a^2}Dt_1\right)\right] \times \sin\frac{\pi n r}{a}\exp\left[-\frac{\pi^2 n^2}{a^2}D(t-t_1)\right]. \quad (8)$$

With equation

$$\sum_{n=1}^{\infty}\frac{(-1)^n}{n^3}\sin\frac{\pi n r}{a} = -\frac{\pi^3}{12}\,\frac{r}{a}\left(1-\frac{r^2}{a^2}\right), \quad (9)$$

it is evident that the expressions (7) and (8) for c_1 and c_2, respectively, represent solutions of systems (1)–(4).

The average (over volume) values of the concentrations $\bar{c}_1$ and $\bar{c}_2$ are defined as:

$$\bar{c}_k(t) = \frac{3}{a^3}\int_0^a c_k(r,t)r^2\,\mathrm{d}r \quad (k=1,2). \quad (10)$$

From (7), (8) and (10) we have:

$$\bar{c}_1(t) = \frac{\gamma a^2}{15D}\left\{1-\frac{90}{\pi^4}\sum_{n=1}^{\infty}\frac{1}{n^4}\exp\left(-\frac{\pi^2 n^2}{a^2}Dt\right)\right\}, \quad (11)$$

$$\bar{c}_2(t) = \frac{6\gamma a^2}{D\pi^4}\sum_{n=1}^{\infty}\frac{1-\exp\left(-\frac{\pi^2 n^2}{a^2}Dt_1\right)}{n^4} \times \exp\left[-\frac{\pi^2 n^2}{a^2}D(t-t_1)\right]. \quad (12)$$

As follows from formula (11), $\bar{c}_1$ runs parallel with time t at low t ($t \ll a^2/D$) and saturates at large t ($\bar{c}_1 = \gamma a^2/(15D)$ in the limit of $t \to \infty$). As follows from formula (12), $\bar{c}_2$ decreases with rising t.

4 Amorphization due to accumulation of point defects in irradiated nanocrystalline solids

Let us analyze amorphization processes in irradiated nanocrystalline solids, using the functions c_1 and c_2 obtained above. To do so, following the approach [29, 33, 34], we assume that amorphization (crystal-to-glass transformation) occurs in a nanocrystalline solid when the total energy of both grain boundaries and irradiation-produced point defects in the solid reaches its critical value equal to the difference ΔE_{am} in the energy between the amorphous and defect-free crystal phases. In the framework of the approach discussed, the criterion for energetically favorable amorphization reads:

$$E_{\mathrm{GB}} + E_{\mathrm{el}} > \Delta E_{\mathrm{am}}. \quad (13)$$

Here E_{GB} is the energy of grain boundaries, and E_{el} is the elastic energy of point defects. In the model of ball-like nanograins, $E_{\mathrm{GB}} = N\omega S$, where N denotes the number of nanograins, S the sum area of grain boundaries surrounding one nanograin, and ω the mean specific energy (per unit area) of grain boundaries. The energy $E_{\mathrm{el}} = cW_{\mathrm{p}}VN$, where W_{p} is the energy of a point defect, c is the absolute concentration of point defects, and V is the nanograin volume. In the standard model [35] (representing point defects as elastic balls characterized by radius $r_0 + \Delta r$ and inserted into spherical pores characterized by radius r_0), the energy W_{p} is given by the following approximate expression: $W_{\mathrm{p}} = 8\,\pi G r_0(\Delta r)^2$. The energy $\Delta E_{\mathrm{am}} = (G/\alpha)VN$, where α is a material-dependent factor.

In our model of ball-like nanograins, the volume V of a nanograin and the sum area S of its grain boundaries are as follows: $V = (4/3)\pi a^3$ and $S = 4\pi a^2$. With these formulas and those for the energies E_{GB}, E_{el} and ΔE_{am} (see above), (13) can be re-written as $c > c_{\mathrm{crit}}$, where

$$c_{\mathrm{crit}} = \frac{1}{8\,\pi r_0(\Delta r)^2}\left(\frac{1}{\alpha}-\frac{3\,\gamma}{Ga}\right). \quad (14)$$

The concentration of point defects in a nanocrystalline solid under irradiation reaches its maximum value at the end of the irradiation treatment. Therefore, if irradiation-induced amorphization does not occur at the end of the irradiation treatment, it does not occur at all. In these circumstances, the critical condition for amorphization of a nanocrystalline solid is given as: $\bar{c}_1(t_1) > c_{\mathrm{crit}}$. Here $\bar{c}_1(t_1)$ is the concentration of point defects at the end of the irradiation treatment, that is, the maximum defect concentration.

Let us consider separately high- and low-energy irradiation processes. With (11) and (14), the critical condition $\bar{c}_1(t_1) > c_{\mathrm{crit}}$ for amorphization in a nanocrystalline solid under high-energy irradiation, can be re-written as $\tilde{\gamma} > \tilde{\gamma}_{\mathrm{c}}$. Here

$$\tilde{\gamma} = \frac{8\pi r_0(\Delta r)^2\omega^2}{G^2 D}\,\gamma, \quad \tilde{\gamma}_{\mathrm{c}} = \frac{15\,(\tilde{a}-3\alpha)}{\alpha\,\tilde{a}^3 f(t_1,\tilde{a})}, \quad (15)$$

$\tilde{a} = (G/\omega)a$, and

$$f(t_1,\tilde{a}) = 1-\frac{90}{\pi^4}\sum_{n=1}^{\infty}\frac{1}{n^4}\exp\left(-\frac{\pi^2 n^2}{\tilde{a}^2}\,\frac{G^2}{\omega^2}\,Dt_1\right). \quad (16)$$

In the case of low-energy irradiation, we have: $\gamma = 3h\beta/a$. Then the critical condition for amorphization is given as $\tilde{\beta} > \tilde{\beta}_{\mathrm{c}}$, where

$$\tilde{\beta} = \frac{8\pi r_0(\Delta r)^2\omega h}{GD}\,\beta, \quad \tilde{\beta}_{\mathrm{c}} = \frac{5\,(\tilde{a}-3\alpha)}{\alpha\,\tilde{a}^2 f(t_1,\tilde{a})}. \quad (17)$$

For $Dt_1/a^2 \ll 1$, we have $f(t_1,\tilde{a}) \approx 15Dt_1G^2/(\omega^2\tilde{a}^2)$. As a corollary, $\tilde{\gamma}_c(Dt_1/a^2 \ll 1) \approx \omega^2(\tilde{a}-3\alpha)(\alpha G^2 Dt_1\tilde{a})$, $\tilde{\beta}_{\mathrm{c}}(Dt_1/a^2 \ll 1) \approx \omega^2(\tilde{a}-3\alpha)/(3\alpha G^2 Dt_1)$. In the limit of $\tilde{a} \to +\infty$, we find $\tilde{\gamma}_c \to \omega^2/(\alpha G^2 Dt_1)$, $\beta_c \sim \omega^2\tilde{a}/(3\alpha G^2 Dt_1)$. In the limit of $t_1 \to +\infty$, we have $f(t_1,\tilde{a}) \to 1$. In these circumstances, the critical condition for amorphization is $\tilde{\gamma} > 15\,(\tilde{a}-3\alpha)/(\alpha\,\tilde{a}^3)$ in the case of high-energy irradiation, and $\tilde{\beta} > 5\,(\tilde{a}-3\alpha)/(\alpha\,\tilde{a}^2)$ in the case of low-energy irradiation.

(In the beginning of irradiation treatment ($t_1 = 0$), we have $f(t_1,\tilde{a}) = 0$. With this equation, the critical conditions for amorphization, $\tilde{\gamma} > \tilde{\gamma}_{\mathrm{c}}$ and $\tilde{\beta} > \tilde{\beta}_{\mathrm{c}}$, are reduced to the inequality: $\tilde{a} < 3\alpha$. In the situation discussed, amorphization occurs due to the contribution E_{GB} of grain boundaries to the energy of the nanocrystalline state. This situation is realized, for

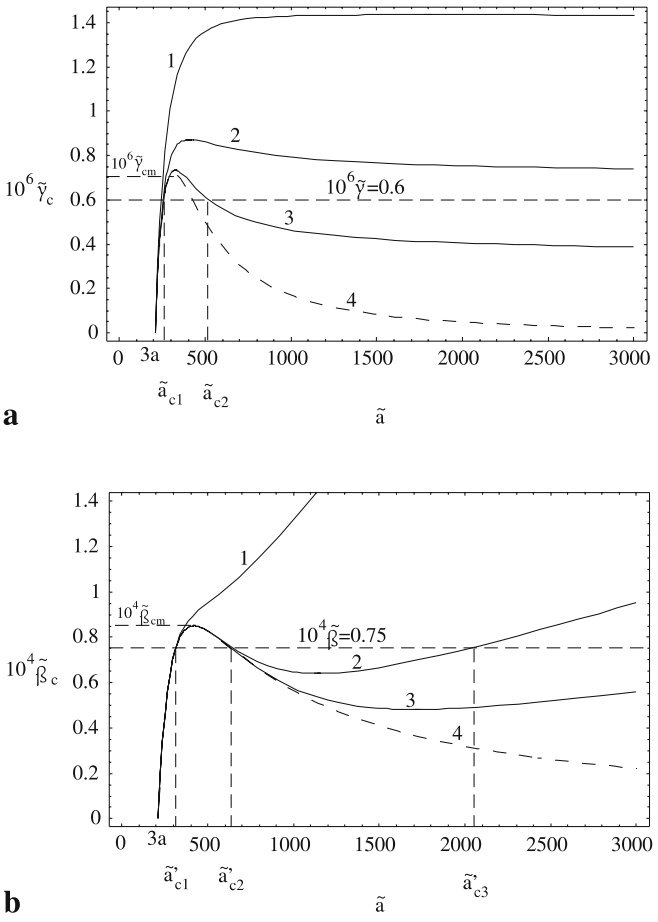

FIGURE 2 Dependences of parameters $\tilde{\gamma}_c$ (**a**) and $\tilde{\beta}_c$ (**b**) on the non-dimensional nanograin radius $\tilde{a}$, for $\alpha = 70$. (**a**) $\omega^2 Dt_1/G^2 = 10^4$, 2×10^4, 4×10^4 and ∞ (curves 1, 2, 3 and 4, respectively). (**b**) $\omega^2 Dt_1/G^2 = 5\times10^4$, 2×10^5, 4×10^5 and ∞ (curves 1, 2, 3 and 4, respectively). These dependences separate the parameter regions where amorphization is energetically unfavorable and favorable, respectively

instance, in ball-milled nanocrystalline solids where severe plastic deformation causes both the formation of new grain boundaries and thereby grain refinement; see, e.g., [36–39]. When the energy of grain boundaries reaches the difference ΔE_{am} in the energy between the amorphous and defect-free crystal phases (in our terms, when $\tilde{a} < 3\alpha$), amorphization occurs in ball-milled nanocrystalline solids. This situation has been theoretically described in the framework of the theormodynamic approach by Desre [34].)

The dependences $\tilde{\gamma}_c(\tilde{a})$ and $\tilde{\beta}_c(\tilde{a})$, calculated with the help of (15)–(17), are shown in Fig. 2, for $\alpha = 70$ and different values of parameter $\omega^2 Dt_1/G^2$. These dependences separate the parameter regions where amorphization is energetically unfavorable and favorable, respectively. As follows from Fig. 2, for $\tilde{a} < 3\alpha$, amorphization is energetically favorable at any values of $\tilde{\gamma}$ (or $\tilde{\beta}$) and t_1. For $\tilde{a} > 3\alpha$, the range ($\tilde{\beta}$, $\tilde{a}$) (or ($\tilde{\gamma}$, $\tilde{a}$)) in which amorphization is energetically favorable, expands with rising time t_1 of the irradiation treatment. In the case of high-energy irradiation, for large values of $\tilde{a}$, the critical parameter $\tilde{\gamma}_c$ approaches the constant value $\omega^2/(\alpha G^2 Dt_1)$ (see Fig. 2a). For small enough t_1 (curve 1 in Fig. 2a), $\tilde{\gamma}_c$ monotonously increases with rising $\tilde{a}$. In doing so, for a given $\tilde{\gamma}$, amorphization is energetically favorable provided $\tilde{a}$ is lower than some critical value. For large values of t_1 (see curves 2 and 3 in Fig. 2a), each of the dependences $\tilde{\gamma}_c$ has one maximum $\tilde{\gamma}_c = \tilde{\gamma}_{cm}(t_1)$. For $\tilde{\gamma} > \tilde{\gamma}_{cm}$, amorphization is energetically favorable at any values of $\tilde{a}$. If $\tilde{\gamma} < \tilde{\gamma}_{cm}$, amorphization can come into play at either sufficiently low ($\tilde{a} < \tilde{a}_{c1}$) or sufficiently large ($\tilde{a} > \tilde{a}_{c2}$) values of $\tilde{a}$. Both $\tilde{a}_{c1}$ and $\tilde{a}_{c2}$ are shown in Fig. 2a, for characteristic values of $\omega^2 Dt_1/G^2 = 2\times10^4$ (corresponding to curve 2) and $\tilde{\gamma} = 0.6\times10^{-6}$.

In the case of low-energy irradiation (Fig. 2b), for large values of $\tilde{a}$, $\tilde{\beta}_c$ is proportional to $\tilde{a}$. In doing so, in the range of small t_1 (see curve 1 in Fig. 2b), $\tilde{\beta}_c$ monotonously grows with rising $\tilde{a}$. For small t_1 and a fixed value of $\tilde{\beta}$, amorphization occurs, if $\tilde{a}$ is lower than some critical value. For large t_1 (see curves 2 and 3 in Fig. 1b), each of the dependences of $\tilde{\gamma}_c$ has one maximum $\tilde{\beta}_c = \tilde{\beta}_{cm}(t_1)$ and one minimum. For $\tilde{\beta} > \tilde{\beta}_{cm}$, amorphization is energetically favorable, if $\tilde{a}$ is not too large. For $\tilde{\beta} < \tilde{\beta}_{cm}$, amorphization occurs either at low $\tilde{a}$ ($\tilde{a} < \tilde{a}'_{c1}$) or in the range: $\tilde{a}'_{c2} < \tilde{a} < \tilde{a}'_{c3}$. Values of $\tilde{a}'_{c1}$, $\tilde{a}'_{c2}$ and $\tilde{a}'_{c3}$ are shown in Fig. 2b, for $\omega^2 Dt_1/G^2 = 2\times10^5$ (corresponding to curve 2) and $\tilde{\beta} = 0.75\times10^{-4}$. In the limit of $t_1 \to \infty$ (see curve 4 in Fig. 2b), we have $\tilde{a}'_{c3} \to \infty$. In these circumstances, amorphization is energetically favorable at either sufficiently low $\tilde{a}$ ($\tilde{a} < \tilde{a}'_{c1}$) or sufficiently large $\tilde{a}$ ($\tilde{a} > \tilde{a}'_{c2}$), similar to the situation with high-energy irradiation.

5 Concluding remarks

In this paper, a theoretical model has been suggested describing the experimentally detected phenomena of the enhancement of irradiation-induced amorphization [17, 18] and instability of irradiation-induced defects [15, 16] in nanocrystalline solids. The model takes into account such specific structural features of nanocrystalline solids as the presence of high-density ensembles of grain boundaries and nanoscale size of crystallites (nanograins). In the framework of the model, it has been shown that the accumulation of point defects in irradiated nanocrystalline solids is either enhanced or hampered, compared to conventional coarse-grained polycrystals. This variety in the behavior occurs due to the competing effects of grain boundaries whose volume fraction is extremely large in nanocrystalline solids. On the one hand, grain boundaries are characterized by excess energy (compared to that of grain-boundary-free crystals) which provides a shift in the energetics of amorphization and thereby enhances irradiation-induced amorphization. On the other hand, grain boundaries act as effective sinks of irradiation-produced point defects, in which case grain boundaries hamper amorphization. If the first factor is dominant, nanocrystalline solids under irradiation treatment exhibit the enhanced ability to solid state amorphizing transformations. If the second factor is dominant, nanocrystalline solids are resistant to irradiation-induced amorphization. The competition between the above effects of grain boundaries on irradiation-induced damage and amorphization processes is responsible for the specific behavior of nanocrystalline solids under irradiation. The suggested concept of the competing effects of grain boundaries on irradiation-induced damage and amorphization processes in the nanocrystalline matter naturally explains the controversial experimental data [15–18] in this area.

The suggested model gives a first approximation description of irradiation-induced amorphization in nanocrystalline solids. In doing so, the model describes homogeneous amorphization under irradiation. At the same time, irradiation-induced amorphization in conventional coarse-grained polycrystalline and microscale composite solids often occurs as a heterogeneous process; see, e.g., [4, 5, 10, 19, 40] and references therein. In general, heterogeneous amorphization processes induced by either irradiation, severe plastic deformation or local stress field inhomogeneities are highly sensitive to the presence of defects, interfaces and stress field distribution in pre-existent crystals [40–47]. Therefore, an adequate description of such heterogeneous amorphization processes in nanocrystalline solids should take into account the interface and nanoscale effects on point defect evolution (as with the situation analyzed in this paper), the role of defects and interfaces as stress sources (enhancing the heterogeneous amorphization), and the role of interphase crystal-glass boundaries (providing a shift in the energetics [48, 49] and thus hampering heterogeneous amorphization). In this context, approximate results of the model suggested in this paper can be effectively used in further theoretical and experimental studies of irradiation-, deformation- and stress-induced amorphization processes in nanocrystalline bulk solids, films and coatings.

ACKNOWLEDGEMENTS The work was supported, in part, by the Office of US Naval Research (grant N00014-01-1-1020), INTAS (grant 03-51-3779), Russian Science Support Foundation, Russian Academy of Sciences Program "Structural Mechanics of Materials and Construction Elements", St. Petersburg Scientific Center, "Integration" Program (grant B0026), and St. Petersburg Government (grant PD04-1.10-9).

REFERENCES

1 C.C. Berndt, T.E. Fischer, I.A. Ovid'ko, G. Skandan, T. Tsakalakos (Eds.): *Nanomaterials for Structural Applications*, MRS Proc. Vol. 740 (MRS, Warrendale 2003)
2 T. Tsakalakos, I.A. Ovid'ko, A.K. Vasudevan (Eds.): *Nanostructures: Synthesis, Functional Properties and Applications*, NATO Science Ser. (Kluwer, Dordrecht 2003)
3 I.A. Ovid'ko, C.S. Pande, R. Krishnamoorti, E. Lavernia, G. Skandan (Eds.): *Mechanical Properties of Nanostructured Materials and Nanocomposites*, MRS Symp. Proc., Vol. 791 (MRS, Warrendale 2004)
4 R.D. Goldberg, J.S. Williams, R.G. Elliman: Phys. Rev. Lett. **82**, 771 (1999)
5 E. Glaser, T. Fehlhaber, B. Breeger: Nucl. Instr. Meth. Phys. Res. B **148**, 426 (1999)
6 A. Plewnia, B. Heinz, P. Ziemann: Nucl. Instr. Meth. Phys. Res. B **148**, 901 (1999)
7 S.X. Wang, G.R. Lumpkin, L.M. Wang, R.C. Ewing: Nucl. Instr. Meth. Phys. Res. B **166–167**, 293 (2000)
8 T. Aruga, Y. Katano, T. Ohmichi, S. Okayashi, Y. Kazumata: Nucl. Instr. Meth. Phys. Res. B **166–167**, 913 (2000)
9 S.X. Wang, L.M. Wang, R.C. Ewing: Nucl. Instr. Meth. Phys. Res.B **175–177**, 615 (2001)
10 J.K.N. Lindner, M. Haberlen, M. Schmid, W. Attenberger, B. Stritzker: Nucl. Instr. Meth. Phys. Res. B **186**, 206 (2002)
11 S. Utsunomiya, L.M. Wang, R.C. Ewing: Nucl. Instr. Meth. Phys. Res. B **191**, 600 (2002)
12 J. Lian, X.T. Zu, K.V.G. Kutty, J. Chen, L.M. Wang, R.C. Ewing: Phys. Rev. B **66**, 054 108 (2002)
13 F. Gao, W.J. Weber: Phys. Rev. B **66**, 024 106 (2002)
14 J. Nord, K. Nordlund, J. Keinonen: Phys. Rev. B **65**, 165 329 (2002)
15 M. Rose, G. Gorzawski, G. Miehe, A.G. Balogh, H. Hahn: Nanostruct. Mater. **127–128**, 119 (1995)
16 M. Rose, A.G. Balogh, H. Hahn: Nucl. Instrum. Meth. Phys. Res. B **127–128**, 119 (1997)
17 A. Meldrum, L.A. Boatner, R.C. Ewing: Phys. Rev. Lett. **88**, 025 503 (2002)
18 A. Meldrum, L.A. Boatner, R.C. Ewing: Nucl. Instr. Meth. Phys. Res. B **207**, 28 (2003)
19 Z.F. Li, B.X. Liu: Appl. Phys. A **75**, 445 (2002)
20 A.T. Motta, A. Paesano, Jr., R.C. Britcher, L. Armaral: Nucl. Instr. Meth. Phys. Res. B **175–177**, 521 (2001)
21 D. Pacifici, E.C. Moreira, G. Franzo, V. Martorino, F. Priolo, F. Iacona: Phys. Rev. B **65**, 144 109 (2002)
22 D. Pacifici, G. Franzo, F. Iacona, F. Priolo: Physica E **16**, 404 (2003)
23 M. Samaras, P.M. Derlet, H. van Swygenhoven, M. Victoria: Phys. Rev. Lett. **88**, 125 505 (2002)
24 H. Swygenhoven, P.M. Derlet, A. Hasnaoui, M. Samaras: In Nanostructures: Synthesis, Functional Properties and Applications, ed. by T. Tsakalakos, I.A. Ovid'ko, A.K. Vasudevan (Kluwer, Dordrecht, 2003), p. 155
25 W. Voegeli, K. Albe, H. Hahn: Nucl. Instr. Meth. Phys. Res. B **202**, 230 (2003)
26 K.E. Sickafus, Hj. Matzke, K. Yasuda, P. Chodak, R.A. Verall, P.G. Lucuta, H.R. Andrews, A. Turos, R. Fromknecht, N. Baker: Nucl. Instr. Meth. Phys. Res. B **141**, 358 (1998)
27 A.P. Sutton, R.W. Balluffi: *Interfaces in Crystalline Materials* (Claredon, Oxford 1995)
28 A.D. Brailsford, R. Bullough: J. Nucl. Mater. **44**, 121 (1972)
29 A.T. Motta, D.R. Olander: Acta Metall. Mater. **38**, 2175 (1990)
30 D.F. Pedraza, Radiat. Eff. **112**, 11 (1990)
31 S.L. Dudarev, A.A. Semenov, C.H. Woo: Phys. Rev. B **67**, 094 103 (2003)
32 J. Crank: *The Mathematics of Diffusion* (Clarendon, Oxford 1993)
33 M.L. Swanson, J.R. Parsons, C.W. Hoelke: Radiat. Effects **9**, 249 (1971)
34 P.J. Desre: Nanostruct. Mater. **8**, 687 (1997)
35 J.P. Hirth, J. Lothe: *Theory of Dislocations* (Wiley, New York 1982)
36 C.C. Koch: Rev. Adv. Mater. Sci. **5**, 91 (2003)
37 C.H. Lee, M. Mori, U. Mizutani: J. Non-Cryst. Solids **117–118**, 733 (1990)
38 Y. Ogino, T. Yamasaki, S. Murayama, R. Sakai: J.Non-Cryst. Solids **117–118**, 737 (1990)
39 U. Y. Bai, C. Michaelson, C. Gente, R. Bormann: Phys. Rev. B **63**, 064 202 (2001)
40 W.J. Weber: Nucl. Instr. Meth. Phys. Res. B **166–167**, 98 (2000)
41 H.W. Sheng, E. Ma: Phys. Res. B **63**, 224 205 (2001)
42 E. Ma: Phys. Res. B **49**, 931 (2003)
43 I.A. Ovid'ko, A.B. Reizis: J. Phys. D **32**, 2833 (1999)
44 M.Yu. Gutkin, I.A. Ovid'ko: Phys. Rev. B **63**, 064 515 (2001)
45 M. Nagumo, T. Ishikawa, T. Endoh, Y. Inoue: Scr. Mater. **49**, 837 (2003)
46 J.Y. Huh, S.J. Moon: Thin Solid Films **377–378**, 611 (2000)
47 M.Y. Gutkin, I.A. Ovid'ko: *Plastic Deformation in Nanocrystalline Materials* (Springer, Berlin, New York, 2004)
48 R. Benedictus, A. Bottger, E.J. Mittenmejer: Phys. Rev. B **54**, 9109 (1996)
49 I.A. Ovid'ko: Phil. Mag. Lett. **79**, 709 (1999)